Learning Real-World Acrobatic Flight from Human Preferences

Colin Merk*,1, Ismail Geles*,1, Jiaxu Xing[1], Angel Romero[1], Giorgia Ramponi[2], and Davide Scaramuzza[1]

***Abstract*—Preference-based reinforcement learning (PbRL) enables agents to learn control policies without requiring manually designed reward functions, making it well-suited for tasks where objectives are difficult to formalize or inherently subjective. Acrobatic flight poses a particularly challenging problem due to its complex dynamics, rapid movements, and the importance of precise execution. In this work, we explore the use of PbRL for agile drone control, focusing on the execution of dynamic maneuvers such as powerloops. Building on Preference-based Proximal Policy Optimization (Preference PPO) [1], we propose *Reward Ensemble under Confidence* (REC), an extension to the reward learning objective that improves preference modeling and learning stability. Our method achieves 88.4% of the shaped reward performance, compared to 55.2% with standard Preference PPO. We train policies in simulation and successfully transfer them to real-world drones, demonstrating multiple acrobatic maneuvers where human preferences emphasize stylistic qualities of motion. Furthermore, we demonstrate the applicability of our probabilistic reward model in a representative MuJoCo environment for continuous control. Finally, we highlight the limitations of manually designed rewards, observing only 60.7% agreement with human preferences. These results underscore the effectiveness of PbRL in capturing complex, human-centered objectives across both physical and simulated domains.**

***Index Terms*—Reinforcement Learning, Machine Learning for Robot Control, Aerial Systems: Perception and Autonomy**

I. Introduction

Autonomous drones capable of executing dynamic and agile maneuvers have become a benchmark for progress in robotics, with applications ranging from high-speed navigation [2] and search-and-rescue to inspection [3]. Reinforcement learning (RL) has shown promise in enabling such high-performance control policies, even surpassing expert human pilots in competitive environments [2]. However, a persistent challenge in applying RL to real-world tasks is the design of effective reward functions.

Reward design is not only time-consuming and task-specific, but it also introduces a fundamental bottleneck: many tasks—particularly those involving aesthetics, subjective quality, or high-level intent—are difficult or even impossible to express with a well-defined reward function. This limitation is especially critical in acrobatic flight maneuvers, where desirable behavior may depend on human preferences over trajectory smoothness, timing, or style.

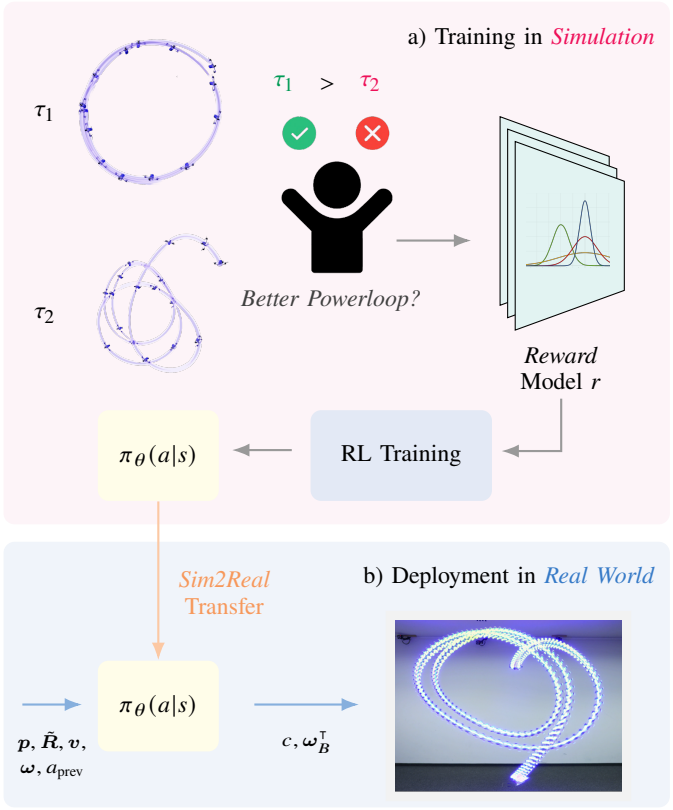

Fig. 1. Learning acrobatic flight from human preferences. (a) In simulation, trajectory pairs (τ_1, τ_2) are shown to a preference annotator to collect preference labels, which are used to train an ensemble of reward models with uncertainty estimation. A policy is then trained with reinforcement learning using the learned reward model. (b) The resulting policy is zero-shot transferred to the real world to execute acrobatic maneuvers.

To address this, preference-based reinforcement learning (PbRL) has emerged as a compelling alternative. Rather than specifying explicit rewards, PbRL infers a reward function from human comparisons between trajectory segments [4]. This approach enables policy learning for tasks that are hard to define but easy to evaluate by preference. Each acrobatic skill would typically require its own carefully designed reward function in traditional RL, whereas PbRL offers a more general framework that can adapt across different maneuvers without task-specific reward engineering. Unlike imitation learning, which requires high-quality demonstrations, PbRL only needs human evaluators to compare behaviors, enabling learning beyond the evaluator's own skill level.

Despite the promise of PbRL, its application in real-world robotics has been limited. Most prior work has focused on simulation, and applications to physical systems, particularly agile drones, remain scarce. Existing methods also tend to overlook the uncertainty inherent in human preferences, which can lead to instability or suboptimal learning when feedback is noisy or sparse.

*These authors contributed equally to this work.

[1] These authors are with the Robotics and Perception Group, University of Zurich, Switzerland (http://rpg.ifi.uzh.ch).
Contact: geles@ifi.uzh.ch

[2]Giorgia Ramponi is with the Autonomous Learning and Predictive Intelligence Lab, University of Zurich, Switzerland.

This work was supported by the European Union's Horizon Europe Research and Innovation Programme under grant agreement No. 101120732 (AUTOASSESS) and the European Research Council (ERC) under grant agreement No. 864042 (AGILEFLIGHT).

In this work, we apply PbRL to the domain of acrobatic drone flight and propose *Reward Ensemble under Confidence* (REC), an extension to the existing Preference-based PPO [1]. Our approach introduces an ensemble-based reward model that accounts for uncertainty in human preferences, significantly improving the training performance.

The key insight behind REC is to explicitly model the probabilistic nature of human feedback, allowing the learning process to better capture ambiguity in preferences [5], avoid overfitting to inconsistent signals, and encourage exploration in regions with high uncertainty captured by an ensemble reward model. This results in more stable training and better policy performance under limited supervision.

We validate our approach through both simulation and real-world experiments. In particular, we train drones to perform continuous powerloop maneuvers and other acrobatic flight skills where human raters express stylistic preferences. Our method achieves 88.4% of the ground-truth reward performance in simulation, compared to 55.2% for standard Preference PPO. We demonstrate successful sim-to-real transfer and further evaluate our reward model in a representative MuJoCo environment. Additionally, we highlight the misalignment between human judgment and hand-crafted rewards, which agree only 60.7% of the time. Our results show that REC Preference PPO can effectively learn expressive and agile flight behaviors using only human preference feedback, demonstrating the feasibility of preference-based learning in complex, agile robotic domains.

II. Related Works

Preference-Based Reinforcement Learning. Preference-based reinforcement learning (PbRL) enables agents to learn policies directly from human-provided comparisons between trajectory segments, bypassing the need for manually designed reward functions. This approach was introduced by [4] and has since inspired numerous advances. Furthermore, limitations in time and sample efficiency have been mitigated through approaches that actively generate pairwise comparisons guided by information gain [6], by selecting batches of comparison pairs [7], and active volume removal [8]. Recent efforts include enhancing exploration efficiency through unsupervised pretraining [9], incorporating transformer-based reward models to capture temporal and non-Markovian aspects of human feedback [10], and exploring implicit reward learning via Q-functions without explicitly modeled rewards [11].

Real-World Deployments of PbRL. Despite its success in simulation, PbRL has seen limited application in real-world robotics, though recent studies show growing interest. One line of research improves sample efficiency by leveraging pre-trained preference models from prior tasks, enabling adaptation to novel tasks on robotic manipulators [12], or using priors obtained from pre-trained LLMs for higher quality candidates in PbRL to achieve expressive behaviors on a quadruped [13]. Another approach combines demonstrations with preference queries to address the inefficiencies of standard PbRL and the limitations of inverse reinforcement learning [14].

Reinforcement Learning in Quadrotor Control. Reinforcement learning has significantly advanced quadrotor control capabilities, with remarkable successes in drone racing [2], [15], robust maneuvering under disturbances [16], and agile flight tasks [17], [18]. Recently, some of the works have even achieved vision-based RL without using any state information [19], [20]. However, most of these methods rely on manually engineered reward functions. Despite these successes, there is a notable absence of PbRL methods explicitly applied to quadrotor control tasks. Our research addresses this critical gap by applying PbRL to acrobatic drone maneuvers, demonstrating both simulation efficacy and real-world feasibility purely based on human preference signals.

III. Methodology

A. Preliminaries

We consider a traditional RL setting in which an agent interacts with an environment. The agent receives an observation o_t from the environment, while taking an action a_t in the environment. For each observation-action pair (o_t, a_t), the agent receives a reward $r_t = r(o_t, a_t)$. In traditional RL, this reward is provided by a hand-crafted set of rules. In PbRL, we use no hand-crafted rewards but a learned reward model instead, which is trained using preference labels obtained from ranking pairs of trajectories. In Online PbRL, these preference labels are collected by repeatedly presenting pairs of trajectories to a human user, who selects the preferred one. This labeling process alternates with policy optimization to iteratively improve the agent's behavior.

Trajectory. We denote a trajectory τ as a sequence of observation–action pairs (o_i, a_i) of length N:

$$\tau = \big((o_1, a_1), (o_2, a_2), \ldots, (o_N, a_N)\big),$$

where o_i is the observation at timestep i and a_i the corresponding action. The total reward of a trajectory $r(\tau)$ is the sum of the rewards at each timestep:

$$r(\tau) = \textstyle\sum_{i=1}^{N} r_i.$$

The reinforcement learning objective can be formalized as maximizing the expected sum of discounted rewards:

$$\max_{\pi} \mathbb{E}_{\tau\sim\pi}\left[r(\tau)\right] = \max_{\pi} \mathbb{E}_{\tau\sim\pi}\left[\textstyle\sum_{i=1}^{N} \gamma^i r_i\right],$$

where π denotes the policy, $\tau \sim \pi$ represents trajectories sampled from the policy, and $\gamma \in [0, 1]$ is the discount factor.

B. Preference-based Reinforcement Learning

To formalize preference-based reinforcement learning, we first define the concepts of *Preference* and *Preference Modeling*, *Cross Entropy Loss*, and *Synthetic Preference Generation*.

Preference. A preference label $p \in [0, 1]$ is assigned by a *judge* to a pair of trajectories, reflecting the relative preference between them. We assume that preferences are determined by an underlying reward function $r : \tau \to \mathbb{R}$, where

$$p(\tau_1, \tau_2) = \begin{cases} 0, & \text{if } r(\tau_1) > r(\tau_2), \\ 0.5 & \text{if } r(\tau_1) = r(\tau_2), \\ 1, & \text{if } r(\tau_1) < r(\tau_2). \end{cases}$$

Preference Modeling. A commonly used model of human judgment, as is also being done in [4], is viewing the reward r of a trajectory τ as a latent variable that determines the choices of the human. More precisely, the probability of preferring one trajectory over the other is given by the softmax of the two rewards,

$$\hat{p}(\tau_1 > \tau_2) = \frac{\exp(\hat{r}_1)}{\exp(\hat{r}_1) + \exp(\hat{r}_2)},$$

which is known as the Bradley–Terry (BT) model. In our notation, we refer to a predicted variable by $\hat{x}$, whereas ground truth variables are referred to as x.

Cross Entropy Loss. In Preference PPO [1], the reward model $\hat{r}$ is optimized by minimizing the cross entropy loss between the BT model predictions and the true labels, using the following loss:

$$\text{loss}(\hat{r}) = -\sum_{(\tau_1^i, \tau_2^i, p^i) \in D} \Big[p^i \cdot \log(\hat{p}(\tau_1^i > \tau_2^i)) + (1 - p^i) \cdot \log(\hat{p}(\tau_2^i > \tau_1^i)) \Big].$$

Synthetic Preference Generation. To assess the performance of our preference-based RL method, we use synthetic preferences, which serve as an oracle representing preferences based on the total handcrafted reward of each compared trajectory in the training environment [4]. The preferred trajectory is the one that achieves a higher reward in the given task. The detailed reward functions of each environment are described in Appendix V-A.

1) Unsupervised Pretraining:

As presented in [9] the pretraining step is used to improve the initial exploration of the policy. In preference-based learning, this is especially useful, as there is no guidance for the policy before the reward model has been trained. To train the reward model, some labeled trajectories are necessary. To encourage exploration, an intrinsic reward is given based on the state entropy $H(s) = \mathbb{E}_{s \in p(s)}[log(p(s))]$. As this is intractable, a particle-based entropy estimator [21] is used:

$$\hat{H}(s) \sim \sum_i log(\|s_i - s_i^k\|).$$

Finally, the intrinsic reward for unsupervised exploration r^{int} is given by the distance to the k-th nearest neighbor of the current state s_t:

$$r^{int}(s_t) = log(\|s_t - s_t^k\|).$$

2) Query and Reward Training Scheduling:

The process of collecting new preferences, also known as querying, and retraining the reward predictor follows the same schedule: the reward model is retrained every time new preferences are gathered.

These schedules are specified in terms of n_{steps}, which represents the number of time-step interactions between the reinforcement learning agent and the environment. We define an epoch as the interval between two consecutive instances of preference collection and reward model retraining. Consequently, the epoch counter increments each time the reward model is updated. The hyperparameters for the preference-based methods are listed in Fig B2 in Appendix V-B.

3) Query Selection:

We select and pair trajectories for preference comparisons using three distinct heuristics. Each method contributes one-third of the total pairs, and each trajectory is used at most once.

Random. The pairs were selected at random, which is used as the default for the first pairing phase where the reward model has not been trained yet.

Ensemble Disagreement. For this pairing method, all possible pairs are generated with the available trajectories. Then, each pair is given a preference label for each ensemble reward prediction – in our case, this would give 5 labels to each pair. Finally, to get the desired pairs, we sort the pairs in descending order by the number of ensembles that contradict each other and select the highest disagreement pairs so that no trajectory is repeated.

Current with previous epoch. Here, "epoch" refers to the interval between two reward retraining phases. For this method, we pair a trajectory that was generated between the current state and the last reward training with a trajectory that was generated before the last reward retraining.

C. REC Preference PPO

In this section, we introduce REC, which extends Preference PPO by explicitly modeling uncertainty in the predicted reward. The methodological differences lie in the loss function for the reward model, the ensemble reward aggregation, and the resetting strategy for the reward model.

1) Loss Function:

Probabilistic Cross Entropy Loss. To derive this loss, we first assume that our reward model predicts a reward sampled from a normal distribution at every time step:

$$r(o_t, a_t) \sim \mathcal{N}\big(r_{\text{mean}}(o_t, a_t), r_{\text{std}}(o_t, a_t)\big).$$

Following this, the reward for the whole trajectory is given by

$$r(\tau) \sim \sum_t \mathcal{N}\big(r_{\text{mean}}(o_t, a_t), r_{\text{std}}(o_t, a_t)\big).$$

This represents the sum of samples drawn from Gaussians with given means and standard deviations. We can rewrite this as:

$$r(\tau) \sim \mathcal{N}\left(\sum_t r_{\text{mean}}(o_t, a_t), \sqrt{\sum_t r_{\text{std}}(o_t, a_t)^2}\right) = \mathcal{N}\Big(r_{\text{mean}}(\tau), r_{\text{std}}(\tau)\Big).$$

Given the distribution for the trajectory reward $r(\tau)$, we can model the preference between two trajectories. Here, Φ denotes the cumulative distribution function (CDF), which gives the probability that a sample from $r(\tau_1)$ is larger than one from $r(\tau_2)$:

$$p(\tau_1 > \tau_2) = \Phi\left(\frac{r_{\text{mean}}(\tau_1) - r_{\text{mean}}(\tau_2)}{\sqrt{r_{\text{std}}(\tau_1)^2 + r_{\text{std}}(\tau_2)^2}}\right).$$

Finally, we derive the preference loss by minimizing the cross-entropy with respect to this probabilistic preference given by

$$\text{loss}(\hat{r}) = -\sum_{(\tau_1^i,\tau_2^i,p^i)\in D} \Big[p^i \log \hat{p}(\tau_1^i > \tau_2^i) + (1-p^i)\log\left(1-\hat{p}(\tau_1^i > \tau_2^i)\right)\Big].$$

Standard Deviation Target Loss. To encourage more stable standard deviation estimates across ensemble members, we introduce an additional loss term. This term penalizes the squared error between a target standard deviation σ_{target} and the mean standard deviation across all timesteps in the preference dataset, $\bar{\sigma}$:

$$\text{loss}_\sigma = (\bar{\sigma} - \sigma_{target})^2.$$

2) Reward Aggregation: For the reward model, we use an ensemble of multi-layer perceptrons (MLPs). The inputs are the current action and observation (a_t, o_t) and the output of each ensemble member is the predicted reward $r^i_{t,pred}$ at time t. We implement a noisy aggregation method that increases the reward in regions of high uncertainty, following the approach of [22]:

$$r^{\text{agg}}_{t,\text{pred}} = \frac{1}{n}\sum_{i=1}^{n} r^i_{t,\text{pred}} + |X|,$$

where X is drawn as below:

$$X \sim \mathcal{N}\left(0, \sqrt{\frac{1}{n}\sum_{i=1}^{n}\left(r^i_{t,\text{pred}} - \frac{1}{n}\sum_{j=1}^{n} r^j_{t,\text{pred}}\right)^2}\right).$$

3) Ensemble Resetting: Before each reward model retraining, we evaluate each ensemble member separately on the newly added preferences. We then re-initialize the weights of the worst-performing $n_{reset} \in [0, \ldots, n_{ensemble}]$ ensemble members. Unless otherwise specified, we use $n_{reset} = 1$ in our experiments.

D. Evaluation Environments

1) DM Control: We evaluated our method in a standard continuous control simulation environment *walker-walk* from the DM Control Suite [23]. The observation space is composed of joint orientations, height, and velocities, with $o_t \in \mathbb{R}^{24}$. The action space consists of normalized joint torques, $a_t \in \mathbb{R}^6$. We used the implementation provided by Tai et al. [24].

2) Quadrotor Control for Acrobatics: We used Flightmare [25] and Agilicious [26] for training control policies on a simulated quadrotor and deploying them in the real world. The dynamics of the quadrotor are simulated as

$$\dot{\boldsymbol{x}} = \begin{bmatrix} \dot{\boldsymbol{p}}_{\mathcal{WB}} \\ \dot{\boldsymbol{q}}_{\mathcal{WB}} \\ \dot{\boldsymbol{v}}_{\mathcal{W}} \\ \dot{\boldsymbol{\omega}}_{\mathcal{B}} \\ \dot{\boldsymbol{\Omega}} \end{bmatrix} = \begin{bmatrix} \boldsymbol{v}_{\mathcal{W}} \\ \boldsymbol{q}_{\mathcal{WB}} \cdot \begin{bmatrix} 0 \\ \boldsymbol{\omega}_{\mathcal{B}}/2 \end{bmatrix} \\ \frac{1}{m}\left(\boldsymbol{q}_{\mathcal{WB}} \odot (\boldsymbol{f}_{\text{prop}} + \boldsymbol{f}_{\text{aero}})\right) + \boldsymbol{g}_{\mathcal{W}} \\ \boldsymbol{J}^{-1}\left(\boldsymbol{\tau}_{\text{prop}} + \boldsymbol{\tau}_{\text{aero}} - \boldsymbol{\omega}_{\mathcal{B}} \times \boldsymbol{J}\boldsymbol{\omega}_{\mathcal{B}}\right) \\ \frac{1}{k_{\text{mot}}}\left(\boldsymbol{\Omega}_{\text{ss}} - \boldsymbol{\Omega}\right) \end{bmatrix},$$

where the operator $\odot$ denotes quaternion-based rotation, while $\boldsymbol{p}_{\mathcal{WB}}$, $\boldsymbol{q}_{\mathcal{WB}}$, $\boldsymbol{v}_{\mathcal{W}}$, and $\boldsymbol{\omega}_{\mathcal{B}}$ represent the vehicle's position, orientation quaternion, velocity in the inertial frame, and angular rates in the body frame, respectively. The parameter k_{mot} characterizes the motor time constant, with Ω and Ω_{ss} corresponding to current and commanded steady-state motor speeds. Additionally, $\boldsymbol{J}$ represents the vehicle's inertia tensor and $\boldsymbol{g}_{\mathcal{W}}$ is the gravitational acceleration vector. Propulsion and aerodynamic effects are captured through the force and torque terms $\boldsymbol{f}_{\text{prop}}, \boldsymbol{\tau}_{\text{prop}}$ and $\boldsymbol{f}_{\text{aero}}, \boldsymbol{\tau}_{\text{aero}}$, respectively. For computational efficiency during training, we employ a quadratic propeller thrust and torque model enhanced with data-driven corrections following the approach of [2]. This provides both accuracy and computational tractability for reinforcement learning applications. Additional details regarding the simulator implementation can be found in [2], [27].

The policy observations at time t includes the drone's position $p_t \in \mathbb{R}^3$, linear velocity $v_t \in \mathbb{R}^3$, the first two columns of the rotation matrix $R_t \in \mathbb{R}^6$, angular velocity $\omega_t \in \mathbb{R}^3$, and the previous action $a_{t-1} \in \mathbb{R}^4$. The action space consists of collective thrust and body rates (CTBR), denoted as $a_t \in \mathbb{R}^4$. The detailed reward for this environment is described in the Appendix V-A.

IV. Results

A. DM Control Evaluation

We test REC Preference PPO on the *walker-walk* task from DM Control [28] and ablate our additions with respect to Preference PPO. Each method is trained 3 times with different seeds. All runs use the same hyperparameters as in [1] whenever applicable. Finally, all methods use a random sampling scheme for creating the pairs for the preference elicitation. Fig. 2 shows the mean episode reward over the course of the training. During training, the policy is evaluated every 800'000 environment interactions. The evaluation rewards in Table I shows the best average performance achieved.

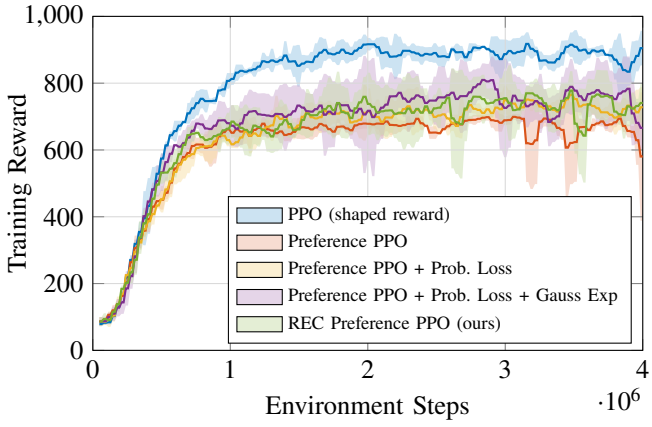

Fig. 2. The average reward while training in the *walker-walk* environment. The shaded area shows the standard deviation. We compare PPO trained with the given environment reward, Preference PPO and our proposed method REC with some ablations. We use 1000 synthetic preferences.

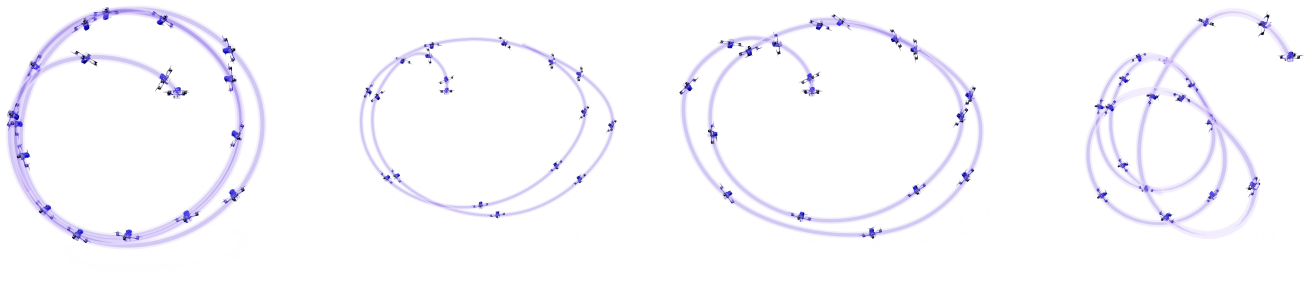

(a) PPO (shaped reward) (b) Preference PPO (synthetic) (c) REC Preference PPO (synthetic, ours) (d) REC Preference PPO (human, ours)

Fig. 3. Stop-motion images of the highest evaluation reward rollout in simulation for different training methods. (a) PPO trained with shaped rewards. (b) Preference PPO trained with 1000 synthetic preferences. (c) REC Preference PPO trained with 1000 synthetic preferences. (d) REC Preference PPO trained with 1000 human-labeled preferences. In each, the trajectory starts red and transitions to green over time.

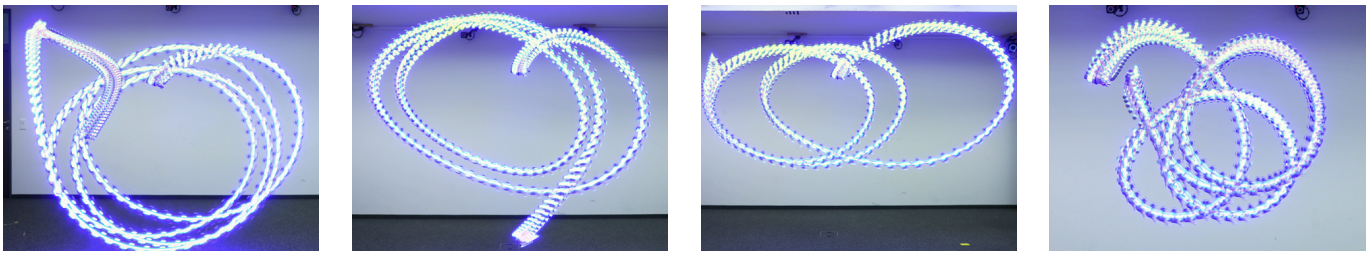

(a) PPO (shaped reward) (b) Preference PPO (synthetic) (c) REC Preference PPO (synthetic, ours) (d) REC Preference PPO (human, ours)

Fig. 4. Deployment results across four training configurations. (a) PPO trained with a manually designed ground-truth reward serves as an upper baseline. (b) Preference PPO trained with synthetic preference labels. (c) Our proposed method REC Preference PPO trained with synthetic labels, showing improved alignment with the intended behavior. (d) Our method trained with real human preferences on the powerloop task.

TABLE I
Maximum evaluation reward (Max. Eval. Rew.) during training in the walker-walk environment. Values represent the highest mean evaluation reward across three runs with different random seeds. The baseline method is Preference PPO and modifications are incrementally introduced to obtain REC Preference PPO.

Method	**Max. Eval. Rew.**
PPO	930.7 ± 12.0
Preference PPO	719.0 ± 9.3
Preference PPO + Prob. Rew. Loss	777.5 ± 66.2
Preference PPO + Prob. Rew. Loss + Rew. Noise	829.4 ± 55.5
Preference PPO + Prob. Rew. Loss + Rew. Noise + Reset Ensemble — (REC)	815.1 ± 43.3

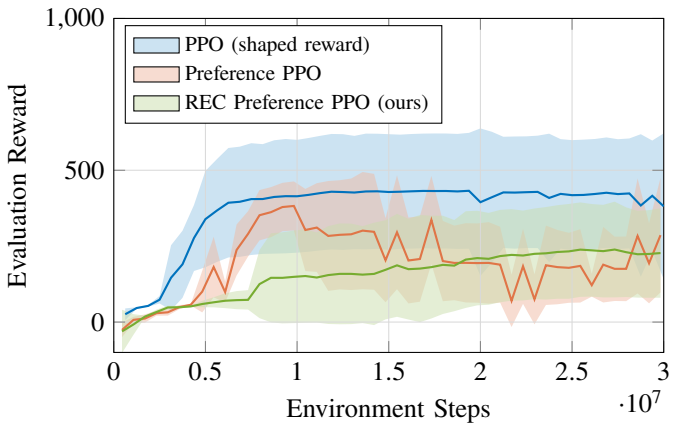

Fig. 5. The average evaluation reward over 3 differently seeded runs is shown here. The shaded area represents the standard deviation. The plot shows the training of the continuous powerloop using PPO with the real reward, Preference PPO with 1000 synthetic labels and REC Preference PPO with 1000 synthetic labels as well.

B. Evaluation on the Quadrotor

We evaluate four training configurations in the Flightmare [25] simulator, which are visualized in Fig. 3. The mean best evaluation reward over three different seeds for each method is shown in Table II. The mean episode reward is visualized in Fig. 5 for training of the quadrotor powerloop, comparing the handcrafted shaped reward with PPO, Preference PPO, and REC Preference PPO using 1000 synthetic preferences, respectively.

C. Real Human Feedback

Finally we test our method REC Preference PPO using a real human annotator. In this experiment, the settings are the same as in the experiments with synthetic preferences, with the only difference being that the feedback is given by the human instead of synthetically through the handcrafted reward.

TABLE II
Maximum evaluation reward (Max. Eval. Rew.) during training of the continuous powerloop. Reported values are the highest mean evaluation reward across three runs with different random seeds. Uncertainty is expressed as the standard deviation.

Method	**Max. Eval. Rew.**
PPO (shaped reward)	432.4 ± 190.8
Preference PPO	238.9 ± 157.5
Preference PPO + Prob. Rew. Loss	281.0 ± 187.4
Preference PPO + Prob. Rew. Loss + Reward Noise	153.9 ± 174.2
Preference PPO + Prob. Rew. Loss + Rew. Noise + Reset Ensemble — (REC)	382.4 ± 80.8

The human judge has the additional option of answering *'I can't tell'*. In this case, the trajectories are discarded and a new pair is prompted at a later point. Due to this, this experiment uses also 1000 preference labels, but in total 1064 comparisons have been shown. The whole training including the labeling took 4 h 43 min. The checkpoint of the policy that is used for evaluation and deployment is chosen by the annotator, instead of the highest reward, as this is assumed to not be available. In Figure 6 the agreement between the human preference and the preference according to the reward model is depicted. Excluding 'tie' predictions, this gives a human accuracy of 60.7%.

Fig. 6. Agreement between the reward model and the human judge.

D. Real World Deployment and Novel Acrobatic Skills

Finally, we deploy the policies that were trained in simulation on a real drone, see Fig. 4. We deploy the policies on a 220 g quadrotor, sending commands as collective thrust and body rates (CTBR). For each experiment that uses synthetic preferences, we choose the checkpoint with the highest evaluation reward. For the experiments using real human feedback, the annotator chooses the checkpoint.

Furthermore, since our method now provides a framework to directly achieve acrobatic drone skills to the desire of human preferences, we are able to learn a novel skill such as a vertical Figure-8 (double powerloop), see Fig. 7, without any changes to the hyperparameters.

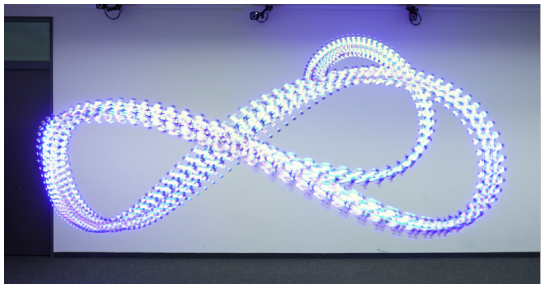

Fig. 7. A novel acrobatic skill defined by the user as vertical Figure-8 (or double powerloop) trained purely from human preferences using REC Preference PPO without any handcrafted reward function.

E. Discussion

Our results demonstrate that both Preference PPO and our proposed method, REC Preference PPO, can successfully learn continuous drone powerloop policies from 1000 synthetic preferences. The probabilistic approach of REC yields a significant performance improvement, achieving an evaluation reward of 382.4, which corresponds to 88.4% of the performance of an agent trained with the shaped reward. In contrast, Preference PPO reached a reward of 238.9, representing only 55.2% of the PPO baseline performance. This substantial improvement demonstrates the effectiveness of incorporating uncertainty quantification into preference-based learning.

Furthermore, we successfully applied our method to learn from 1000 real human preferences for two distinct tasks: the standard powerloop and a novel vertical Figure-8 (double powerloop) acrobatic maneuver specified by the user without requiring any manual reward function design. This demonstrates the practical applicability of our approach to complex, real-world scenarios where reward engineering is challenging or infeasible, and showcases the potential for non-domain experts to directly improve robot skills through intuitive preference feedback rather than requiring specialized knowledge in robotics or control theory.

A particularly noteworthy finding is that a successful policy was learned from human feedback despite achieving only 60.7% agreement with the pre-defined shaped environment reward. This low agreement underscores the inherent difficulty in engineering reward functions that truly capture human intent and highlights the superior ability of preference-based methods to learn from implicit human knowledge and preferences that may be difficult to formalize mathematically.

One limitation of our current approach is the human evaluation process itself, which requires humans to view and compare two animations from the quadrotor simulator for each preference decision. This proved to be time-consuming and the human judgments are inherently viewpoint-dependent, as the perceived quality of acrobatic maneuvers can vary significantly based on the camera angle and perspective from which the flight is observed, potentially affecting the overall learning performance. Moreover, setting up a feasible rendering for such evaluations already presupposes some notion of what the final maneuver should look like, as camera placement and visualization choices strongly bias how trajectories are perceived.

Despite these promising results, our experiments exhibited high variance due to the inherent difficulty of the acrobatic tasks. Agents frequently failed to explore beyond the initial half-flip maneuver, resulting in low evaluation rewards and preventing us from demonstrating statistical significance across all conditions. This exploration challenge represents a common limitation in complex continuous control tasks and suggests that future work could benefit from incorporating more sophisticated exploration strategies or curriculum learning approaches.

V. Conclusion

In this work, we present REC, a probabilistic extension to preference-based reinforcement learning that incorporates uncertainty quantification for training autonomous quadrotors to perform complex acrobatic maneuvers. Our key contributions include: (1) the development of a probabilistic framework that significantly outperforms standard preference-based methods, achieving 88.4% of ground truth reward performance compared to 55.2% for baseline approaches; (2) successful validation on both synthetic and real human preferences across multiple acrobatic tasks; and (3) demonstration that effective policies can be learned even when human preferences show low agreement with engineered reward functions.

The results highlight the potential of probabilistic preference-based learning for complex robotics applications where reward specification is challenging. Our approach successfully learned policies for both standard powerloop and novel vertical Figure-8 maneuvers from human feedback alone, eliminating the need for manual reward engineering. This represents a significant step toward more intuitive and accessible robot training paradigms.

Future work could focus on addressing the high variance in performance through improved exploration strategies, improving the efficiency and quality of human preference collection through reduced viewpoint dependency, conducting larger-scale human studies to establish statistical significance, and extending the approach to a broader range of robotic tasks and domains. The integration of uncertainty quantification into preference-based learning opens promising avenues for developing more robust and human-aligned autonomous systems.

References

[1] K. Lee, L. Smith, A. Dragan, and P. Abbeel, "B-pref: Benchmarking preference-based reinforcement learning," 2021. [Online]. Available: https://arxiv.org/abs/2111.03026

[2] E. Kaufmann, L. Bauersfeld, A. Loquercio, M. Müller, V. Koltun, and D. Scaramuzza, "Champion-level drone racing using deep reinforcement learning," *Nature*, vol. 620, no. 7976, pp. 982–987, Aug. 2023, publisher: Nature Publishing Group. [Online]. Available: https://www.nature.com/articles/s41586-023-06419-4

[3] J. Xing, G. Cioffi, J. Hidalgo-Carrió, and D. Scaramuzza, "Autonomous power line inspection with drones via perception-aware mpc," in *2023 IEEE/RSJ International Conference on Intelligent Robots and Systems (IROS)*. IEEE, 2023, pp. 1086–1093.

[4] P. Christiano, J. Leike, T. B. Brown, M. Martic, S. Legg, and D. Amodei, "Deep reinforcement learning from human preferences," 2023. [Online]. Available: https://arxiv.org/abs/1706.03741

[5] S. Casper, X. Davies, C. Shi, T. K. Gilbert, J. Scheurer, J. Rando, R. Freedman, T. Korbak, D. Lindner, P. Freire, T. T. Wang, S. Marks, C.-R. Segerie, M. Carroll, A. Peng, P. J. Christoffersen, M. Damani, S. Slocum, U. Anwar, A. Siththaranjan, M. Nadeau, E. J. Michaud, J. Pfau, D. Krasheninnikov, X. Chen, L. Langosco, P. Hase, E. Biyik, A. Dragan, D. Krueger, D. Sadigh, and D. Hadfield-Menell, "Open problems and fundamental limitations of reinforcement learning from human feedback," *Transactions on Machine Learning Research*, 2023, survey Certification, Featured Certification. [Online]. Available: https://openreview.net/forum?id=bx24KpJ4Eb

[6] E. Biyik, M. Palan, N. C. Landolfi, D. P. Losey, and D. Sadigh, "Asking easy questions: A user-friendly approach to active reward learning," in *Proceedings of the Conference on Robot Learning*, ser. Proceedings of Machine Learning Research, L. P. Kaelbling, D. Kragic, and K. Sugiura, Eds., vol. 100. PMLR, 30 Oct–01 Nov 2020, pp. 1177–1190. [Online]. Available: https://proceedings.mlr.press/v100/b-iy-ik20a.html

[7] E. Biyik, N. Anari, and D. Sadigh, "Batch active learning of reward functions from human preferences," *ACM Transactions on Human-Robot Interaction*, vol. 13, no. 2, pp. 1–27, 2024.

[8] D. Sadigh, A. D. Dragan, S. S. Sastry, and S. A. Seshia, "Active preference-based learning of reward functions," in *Robotics: Science and Systems*, 2017. [Online]. Available: https://api.semanticscholar.org/CorpusID:12226563

[9] K. Lee, L. Smith, and P. Abbeel, "PEBBLE: Feedback-Efficient Interactive Reinforcement Learning via Relabeling Experience and Unsupervised Pre-training," June 2021, arXiv:2106.05091 [cs]. [Online]. Available: http://arxiv.org/abs/2106.05091

[10] C. Kim, J. Park, J. Shin, H. Lee, P. Abbeel, and K. Lee, "Preference transformer: Modeling human preferences using transformers for rl," 2023. [Online]. Available: https://arxiv.org/abs/2303.00957

[11] J. Hejna and D. Sadigh, "Inverse preference learning: Preference-based rl without a reward function," 2023. [Online]. Available: https://arxiv.org/abs/2305.15363

[12] D. J. H. III and D. Sadigh, "Few-shot preference learning for human-in-the-loop RL," in *6th Annual Conference on Robot Learning*, 2022. [Online]. Available: https://openreview.net/forum?id=IKC5TfXLuW0

[13] J. Clark, J. Hejna, and D. Sadigh, "Efficiently generating expressive quadruped behaviors via language-guided preference learning," *preprint*, 2024.

[14] M. Palan, G. Shevchuk, N. C. Landolfi, and D. Sadigh, "Learning reward functions by integrating human demonstrations and preferences," in *Proceedings of Robotics: Science and Systems*, FreiburgimBreisgau, Germany, June 2019.

[15] Y. Song, A. Romero, M. Mueller, V. Koltun, and D. Scaramuzza, "Reaching the limit in autonomous racing: Optimal control versus reinforcement learning," *Science Robotics*, p. adg1462, 2023. [Online]. Available: https://www.science.org/doi/10.1126/scirobotics.adg1462

[16] A. M. Deshpande, A. A. Minai, and M. Kumar, "Robust deep reinforcement learning for quadcopter control," 2021. [Online]. Available: https://arxiv.org/abs/2111.03915

[17] S. Lupashin, A. Schöllig, M. Sherback, and R. D'Andrea, "A simple learning strategy for high-speed quadrocopter multi-flips," in *2010 IEEE International Conference on Robotics and Automation*. Anchorage, AK: IEEE, May 2010, pp. 1642–1648. [Online]. Available: http://ieeexplore.ieee.org/document/5509452/

[18] J. Xing, I. Geles, Y. Song, E. Aljalbout, and D. Scaramuzza, "Multi-task reinforcement learning for quadrotors," *IEEE Robotics and Automation Letters*, 2024.

[19] I. Geles, L. Bauersfeld, A. Romero, J. Xing, and D. Scaramuzza, "Demonstrating Agile Flight from Pixels without State Estimation," in *Proceedings of Robotics: Science and Systems*, Delft, Netherlands, July 2024.

[20] J. Xing, A. Romero, L. Bauersfeld, and D. Scaramuzza, "Bootstrapping reinforcement learning with imitation for vision-based agile flight," *Conference on Robot Learning*, 2024.

[21] H. Liu and P. Abbeel, "Behavior from the void: Unsupervised active pre-training," 2021. [Online]. Available: https://arxiv.org/abs/2103.04551

[22] X. Liang, K. Shu, K. Lee, and P. Abbeel, "Reward uncertainty for exploration in preference-based reinforcement learning," 2022. [Online]. Available: https://arxiv.org/abs/2205.12401

[23] Y. Tassa, Y. Doron, A. Muldal, T. Erez, Y. Li, D. de Las Casas, D. Budden, A. Abdolmaleki, J. Merel, A. Lefrancq, T. Lillicrap, and M. Riedmiller, "Deepmind control suite," 2018. [Online]. Available: https://arxiv.org/abs/1801.00690

[24] J. J. Tai, M. Towers, and E. Tower, "Shimmy: Gymnasium and PettingZoo Wrappers for Commonly Used Environments," June 2023. [Online]. Available: https://doi.org/10.5281/zenodo.8140744

[25] Y. Song, S. Naji, E. Kaufmann, A. Loquercio, and D. Scaramuzza, "Flightmare: A flexible quadrotor simulator," in *Proceedings of the 2020 Conference on Robot Learning*, 2021, pp. 1147–1157.
[26] P. Foehn, E. Kaufmann, A. Romero, R. Penicka, S. Sun, L. Bauersfeld, T. Laengle, G. Cioffi, Y. Song, A. Loquercio, and D. Scaramuzza, "Agilicious: Open-source and open-hardware agile quadrotor for vision-based flight," *Science Robotics*, vol. 7, no. 67, p. eabl6259, 2022.
[27] L. Bauersfeld, E. Kaufmann, P. Foehn, S. Sun, and D. Scaramuzza, "Neurobem: Hybrid aerodynamic quadrotor model," *RSS: Robotics, Science, and Systems*, 2021.
[28] S. Tunyasuvunakool, A. Muldal, Y. Doron, S. Liu, S. Bohez, J. Merel, T. Erez, T. Lillicrap, N. Heess, and Y. Tassa, "dm control: Software and tasks for continuous control," *Software Impacts*, vol. 6, p. 100022, Nov. 2020. [Online]. Available: http://dx.doi.org/10.1016/j.simpa.2020.100022

APPENDIX

A. Quadrotor Powerloop Shaped Reward

We design a shaped, Markovian reward for the PPO baseline as well as a synthetic judge to enable preference learning for continuous powerloops. The reward consists of three components:

1) Planar Penalty: Encourages movement in the xz-plane using the L1 distance to the plane. The drone's position is given by $\vec{p}_{drone}$, with p_{planar} referring to the drone's position projected onto the circle plane given by the normal $\vec{n}_{circle}$:

$$p_{planar} = |(\vec{p}_{drone} - \vec{c}_{circle}) \cdot \vec{n}_{plane}|_1. \tag{1}$$

2) Circular Motion Reward: Rewards tangential movement along a target circle using saturated planar velocity. The vector $\vec{t}$ refers to the tangent of the circle and $\vec{v}_{circular,sat}$ relates to the drone's velocity projected to the circle's plane and saturated at a maximum value:

$$r_{circ} = \vec{t} \cdot \vec{v}_{circular,sat}. \tag{2}$$

3) Action Regularization: Penalizes high-frequency noise in actions for hardware safety. We consider the actions for body rates ω_{xy}, ω_z, and thrust c:

$$p_{reg,i} = |c_{i,high}| + |c_{i,high}|^2. \tag{3}$$

The total reward is a weighted sum of these components:

$$r_{total} = \alpha \cdot r_{circ} - \beta \cdot p_{planar} - \sum_i \gamma_i \cdot p_{reg,i}, \tag{4}$$

where we use $\alpha = 0.5$, $\beta = 3$, $\gamma_{\omega_{xy}} = \gamma_{\omega_z} = 0.008$, and $\gamma_{\omega_c} = 0.0001$.

B. Hyperparameters

The hyperparameters used in our experiments are summarized in Tables B1 and B2. Table B1 lists the settings for the PPO baseline in both the *walker-walk* and *flightmare* environments. Table B2 provides the corresponding settings for the preference-based methods, including Preference PPO and REC Preference PPO.

TABLE B1
Hyperparameters of the PPO algorithm in the *walker-walk* and *flightmare* environments.

Hyperparameter	**flightmare**	**walker-walk**
n_{envs}	50	32
$n_{\text{timesteps}}$	30M	4M
γ	0.995	0.99
λ_{GAE}	0.95	0.92
n_{epochs}	10	20
n_{steps}	250	500
ϵ_{clip}	0.4	0.4
n_{batch}	12,500	64
$\log \sigma_{\text{init}}$	-0.8	0.0
π_{arch}	[128, 128]	[256, 256, 256]
$\pi_{\text{activation}}$	Tanh	Tanh
c_{entropy}	0.001	0.0

TABLE B2
Hyperparameters of the preference-based algorithms in the *walker-walk* and *flightmare* environments. The pairing method for both environments is 50% ensemble disagreement and 50% random.

Hyperparameter	**flightmare**	**walker-walk**
n_{prefs}	1000	1000
T_{clip}	1.25 s	1.25 s
f_{init} Initial preference fraction	0.2	0.1
n_{query} Preference collection steps	10	10
$\Delta t_{\text{retrain}}$ Reward re-training interval steps	400K	16K
n_{ensemble}	5	3
$d^{\mathcal{R}}_{\text{hidden}}$	256	256
$n^{\mathcal{R}}_{\text{layers}}$	2	2
$\phi^{\mathcal{R}}$	Tanh	Tanh
$n^{\mathcal{R}}_{\text{epochs}}$	100	100
$\eta^{\mathcal{R}}$	0.0003	0.0003